SCIENCE CHINA
Information Sciences

• LETTER •

October 2018, Vol. 61 109302:1–109302:3
https://doi.org/10.1007/s11432-018-9471-3

Single-channel sampling and multi-channel reconstruction AIC via multiple chirp noise sequences

Pengfei SHI[1,2], Hao HUAN[1,2*] & Ran TAO[1,2*]

[1]*School of Information and Electronics, Beijing Institute of Technology, Beijing* 100081*, China;*
[2]*Beijing Key Laboratory of Fractional Signals and Systems, Beijing Institute of Technology, Beijing* 100081*, China*

Received 9 April 2018/Revised 22 May 2018/Accepted 29 May 2018/Published online 2 August 2018

Citation Shi P F, Huan H, Tao R. Single-channel sampling and multi-channel reconstruction AIC via multiple chirp noise sequences. Sci China Inf Sci, 2018, 61(10): 109302, https://doi.org/10.1007/s11432-018-9471-3

Dear editor,
As preliminary implementation of compressed sensing (CS), the analog-to-information converter (AIC) plays an important role in reducing the sampling rate of analog signals via PN sequence [1, 2]. However, it suffers severe reconstruction errors (REs) when acquiring noisy signals prior to measurement in cases with low signal-noise ratio (SNR) [3].

To damp the RE, the adaptive weighted norm constraint is first introduced in [4], which enables the weighted l_1 norm constrained model obtain an accurate approximation of the l_0 norm model. Distilled sensing is used to control the noise folding by designing adaptive measurements to detect and locate weak signals in the additive white Gaussian noise (AWGN) environment [5]. Further, two new-types of decoding procedures are proposed by combining l_1-minimization with either a regularized selective least p-powers or an iterative hard thresholding [6]. Meanwhile, a data pre-processing operation, such as the adaptive selective compressive sampling (ASCS) in [7], is preliminarily considered in the recovery algorithm. These relative studies on the RE are mainly focused on the sparse signal and its noise; however, it is the nonlinear reconstruction matrix that plays the dominant role in the RE [8].

In this study, the single-channel sampling and multi-channel reconstruction (SCS-MCR) AIC scheme is proposed to damp the RE completely with low hardware consumption, as shown in Figure 1(a). In the proposed scheme, the nonlinear reconstruction matrix is approximate to the linear diagonal matrix by the incoherent accumulation in the digital domain.

The proposed model. The proposed SCS-MCR AIC scheme is depicted in Figure 1(a). First, the multiple mixing sequences are superimposed together on the original analog signal $\boldsymbol{x}(t)$. Further, the mixed analog signal is sampled by only one analog-to-digital converter (ADC) after the lowpass filter. Finally, in the digital domain, the recovery signals are accumulated together after they are reconstructed in each channel according to each mixing sequence. The mathematical process is realized as follows.

As shown in Figure 1(a), the original signal $\boldsymbol{x} \in \mathbb{R}^N$ has an s-sparse representation with respect to the basis $\boldsymbol{\Psi}$ if its transform $\boldsymbol{\alpha} \in \mathbb{R}^N$ ($\boldsymbol{x} = \boldsymbol{\Psi\alpha}$) contains at most s ($s \ll N$) nonzero elements. The signal $\boldsymbol{x}$ is modulated by the multiple mixing sequences $\boldsymbol{p}_k = [p_k(1), p_k(2), \ldots, p_k(N)]^{\mathrm{T}}, k = 1, \ldots, K$, so that it is not destroyed by the impulse response $\boldsymbol{h} = [h(1), h(2), \ldots, h(N)]^{\mathrm{T}}$ of the lowpass filter. Finally, it is sampled at the $1/\gamma$ ($\gamma = N/M$) Nyquist sampling (NS) rate with interval T_s. The compressed signal is expressed as follows:

$$\boldsymbol{y} = \sum_{k=1}^{K} \boldsymbol{A}_k(\boldsymbol{\alpha} + \boldsymbol{z}) + \boldsymbol{w}, \tag{1}$$

* Corresponding author (email: huanhao@bit.edu.cn, rantao@bit.edu.cn)

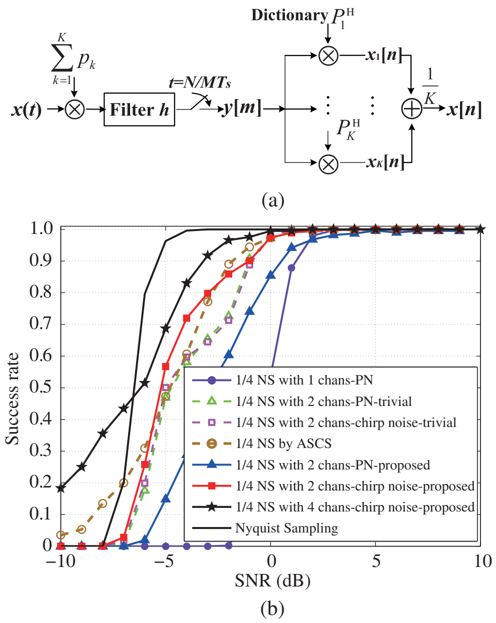

Figure 1 (Color online) (a) Schematic architecture of the proposed SCS-MCR AIC scheme and (b) its recovery performance at 1/4 sub-NS rate.

where $\boldsymbol{y} \in \mathbb{R}^M$ is the measurement vector and $\boldsymbol{A}_k = \boldsymbol{H}\boldsymbol{P}_k\boldsymbol{\Psi} \in \mathbb{R}^{M\times N}$ is the given matrix with $M \leqslant N$. $\boldsymbol{P}_k$ is an $N \times N$ matrix with the diagonal elements of $\boldsymbol{p}_k$ and $\boldsymbol{H}$ is the cyclic shift by row of the lowpass filter $\boldsymbol{h}$ with size of $M \times N$. Both the signal noise $\boldsymbol{z} \in \mathbb{R}^N$ and the measurement noise $\boldsymbol{w} \in \mathbb{R}^M$ are the uncorrelated AWGN, subjected to the Gaussian distribution with $\mathbf{0}$ mean and $\sigma_0^2\boldsymbol{I}$ and $\sigma^2\boldsymbol{I}$ covariances. It is observed that $\boldsymbol{I}$ is the identity matrix and $(\cdot)^{\rm H}$ denotes the conjugate transpose.

After the mixed analog signal is sampled by only one ADC, the compressed signal $\boldsymbol{y}$ is reconstructed by each channel of the digital domain.

$$\begin{cases} \boldsymbol{A}_1^{\rm H}\boldsymbol{y} = \boldsymbol{A}_1^{\rm H}\sum_{k=1}^{K}\boldsymbol{A}_k(\boldsymbol{\alpha}+\boldsymbol{z}) + \boldsymbol{A}_1^{\rm H}\boldsymbol{w}, \\ \qquad\vdots \\ \boldsymbol{A}_K^{\rm H}\boldsymbol{y} = \boldsymbol{A}_K^{\rm H}\sum_{k=1}^{K}\boldsymbol{A}_k(\boldsymbol{\alpha}+\boldsymbol{z}) + \boldsymbol{A}_K^{\rm H}\boldsymbol{w}, \end{cases} \tag{2}$$

with the recovery performance decided by

$$\begin{aligned} \eta_k := & \left\| \boldsymbol{I} - \frac{1}{\gamma}\sum_{l=1}^{K}\boldsymbol{A}_l\boldsymbol{A}_k^{\rm H} \right\|_2 \\ \leqslant & \left\| \boldsymbol{I} - \frac{1}{\gamma}\boldsymbol{A}_k\boldsymbol{A}_k^{\rm H} \right\|_2 + \frac{1}{\gamma}\left\| \sum_{l=1,l\neq k}^{K}\boldsymbol{A}_l\boldsymbol{A}_k^{\rm H} \right\|_2, \end{aligned} \tag{3}$$

where $\|\cdot\|_2$ denotes the standard operator norm on $\mathbb{R}^{M\times M}$. It is observed in [3] that $\|\boldsymbol{I} - (1/\gamma)\boldsymbol{A}_k\boldsymbol{A}_k^{\rm H}\|_2$ is often small because the diagonal elements of $1/\gamma\boldsymbol{A}_k^{\rm H}\boldsymbol{A}_k$ are 1, while the other $\gamma-1$ non-zero elements $1/\gamma$ in each row are randomly distributed. Meanwhile, if there is quasi orthogonality between different mixing sequences $\boldsymbol{p}_k$ and $\boldsymbol{p}_{l,l\neq k}$, $\|\sum_{l=1,l\neq k}^{K}\boldsymbol{A}_l\boldsymbol{A}_k^{\rm H}\|_2$, it will be small enough, yielding η_k close to 0.

Finally, based on the reconstruction scheme discussed in (2), the incoherent accumulation for the sparse signal $\boldsymbol{\alpha}$ is obtained by

$$\begin{aligned} \frac{\sum_{k=1}^{K}\boldsymbol{A}_k^{\rm H}\boldsymbol{y}}{K} = & \frac{\sum_{k=1}^{K}\boldsymbol{A}_k^{\rm H}\sum_{k=1}^{K}\boldsymbol{A}_k}{K}(\boldsymbol{\alpha}+\boldsymbol{z}) \\ & + \frac{\sum_{k=1}^{K}\boldsymbol{A}_k^{\rm H}}{K}\boldsymbol{w}. \end{aligned} \tag{4}$$

It is assumed that the columns of $\boldsymbol{A}_k$ are normalized so that $\|\boldsymbol{A}_{k,t}\|_2 = 1$ for $t = 1,\ldots,N$. For any subset $S \subseteq \{1,\ldots,N\}$, we shall use $\boldsymbol{A}_k(S)$ to denote a submatrix of $\boldsymbol{A}_k$ consisting of the columns $\boldsymbol{A}_k(i)$ columns with $i \in S$. Based on the orthogonal matching pursuit (OMP) algorithm discussed in [9], the partial matching algorithm is proposed for the recovery of the sparse signal in the SCS-MCR AIC scheme using the following steps:

Step 1. Set the index $k = 1$ for $\boldsymbol{A}_k$.

Step 2. Initialize the residual $\boldsymbol{r}_{k,0} = \boldsymbol{y}$, the selected variables $\boldsymbol{A}_k(c_{k,0}) = \emptyset$, and its index $c_{k,0} = \emptyset$. Let the initial iteration counter $i = 1$ with maximum iteration counter I_0.

Step 3. Find the variable $\boldsymbol{A}_{k,t_i}$ that solves the maximization problem $\max_t |\boldsymbol{A}_{k,t}^{\rm H}\boldsymbol{r}_{k,i-1}|$ and add the variable $\boldsymbol{A}_{k,t_i}$ to the set of selected variables. Update $c_{k,i} = c_{k,i-1}\bigcup t_i$.

Step 4. Let

$$\boldsymbol{P}_{k,i} = \boldsymbol{A}_k(c_{k,i})\cdot(\boldsymbol{A}_k(c_{k,i})^{\rm H}\boldsymbol{A}_k(c_{k,i}))^{-1}\cdot\boldsymbol{A}_k(c_{k,i})^{\rm H}$$

be the projection onto the linear space spanned by the elements $\boldsymbol{A}_k(c_{k,i})$, where $(\cdot)^{-1}$ denotes inverse matrix. Update $\boldsymbol{r}_{k,i} = (\boldsymbol{I} - \boldsymbol{P}_{k,i})\,\boldsymbol{y}$.

Step 5. For each channel with $k < K$, if the stopping condition $|r_{k,i}| < \epsilon$ is not achieved and $i = I_0$, set $i = i + 1$ and return to Step 3. If the stopping condition is achieved and $k < K$, set $i = 1$, $k = k + 1$ and return to Step 2. If $k = K$, end the algorithm.

Let $\boldsymbol{A} = \sum_{k=1}^{K}\boldsymbol{A}_k$ and $\boldsymbol{A}^+$ be the pseudo-inverse matrix of $\boldsymbol{A}$. The recovery signal $\hat{\boldsymbol{\alpha}}$ is obtained by averaging the partial matching results in K channels.

$$\hat{\boldsymbol{\alpha}} = \frac{1}{K}\sum_{k=1}^{K}\boldsymbol{A}(c_{k,i})^+\boldsymbol{y}. \tag{5}$$

In the partial matching algorithm, both the real and false targets are reconstructed simultaneously in each channel. Further, the false targets are finally restrained by multi-channel accumulation in (5). The incoherent accumulation is achieved in the digital domain; thus, the proposed SCS-MCR AIC scheme is realized with low hardware consumption, compared with the segment-sliding reconstruction in [10].

Furthermore, in the proposed SCS-MCR AIC scheme, the multiple mixing sequences superimposed on the original analog signal should be separated perfectly in the digital domain, so that the interference among different mixing sequences is as small as possible. Considering this condition, the chirp noise sequence is designed for the proposed SCS-MCR AIC scheme. The discrete chirp noise sequence $\boldsymbol{p}_k = [p_k(0), \ldots, p_k(n), \ldots, p_k(N-1)]^{\mathrm{T}}$ for $k = 1, \ldots, K$ is given by

$$p_k(n) = \mathrm{e}^{\mathrm{j}\pi\mu(n\Delta t)^2 + \mathrm{j}\rho\phi_k(n)}, \tag{6}$$

where μ is the chirp rate, Δt is the NS interval, $\phi_k(n)$ is the pseudo-random phase following the uniform distribution $[0, 2\pi]$, and $\rho \in [0, 1]$ is the phase scale factor. We take $\rho \in [0.4, 0.6]$ in this study. It is observed that the chirp signal in $\boldsymbol{p}_k$ provides the flat power density for the uniform distribution of the original analog signal in the frequency domain, while the pseudo-random phase provides the diversity for the design of the multiple mixing sequences.

Numerical experiments. The following numerical simulations provide the empirical confirmation in the LFM radar. In the AWGN environment, the simulation parameters for the three received random sparse targets are given by $\boldsymbol{x} = g_T(t)a_0\mathrm{e}^{\mathrm{j}\pi\mu t^2}$, a chirp signal with a pulse repetition time (PRT) $T_r = 8$ μs, amplitude $a_0 = 1$, and bandwidth $B = 64$ MHz, where $g_T(t)$ is the pulse shape function with the interval $T = 1$ μs. The proposed SCS-MCR AIC schemes via multiple chirp noise sequences ($\rho = 0.5$) is verified at 1/4 NS rate and we take OMP as our recovery algorithm. For each simulation, 1000 Monte-Carlo runs are performed.

The recovery performance of the proposed SCS-MCR AIC scheme is depicted in Figure 1(b). With a 90% success rate, the dual-channel SCS-MCR AIC via multiple chirp noise sequences has 2 dB gain more than that via multiple PN sequences. Besides, with the increasing channels, the recovery performance of SCS-MCR AIC via multiple chirp noise sequences is approximate to that at the NS rate. Compared with the ASCS scheme in [7], the proposed dual-channel SCS-MCR AIC via multiple chirp noise sequences share the similar recovery performance without modifying the mixing sequences in real time through the estimated noise information. Meanwhile, compared with trivial parallel AIC scheme discussed in [11], the SCS-MCR AIC via multiple chirp noise sequences has similar recovery performance without extra hardware consumption.

Conclusion. In this study, we propose a novel SCS-MCR AIC scheme via multiple chirp noise sequences to damp the RE completely with low hardware consumption. The multiple chirp noise sequences are added together in the analog domain for the original signal and reconstructed by different channels in the digital domain. The numerical experiments demonstrate that the recovery accuracy of sparse signal in the proposed scheme is approximate to that at the NS rate with an increasing number of chirp noise sequences, which is better than that by adaptive selective compressive sampling.

Acknowledgements This work was supported by National Natural Science Foundation of China (Grant Nos. 61501031, 91638205, 61421001, 61331021).

References

1 Yan H C, Xu J, Xia X G, et al. Underwater sonar target imaging via compressed sensing with M sequences. Sci China Inf Sci, 2016, 59: 122308

2 Li L C, Li D J, Pan Z H. Compressed sensing application in interferometric synthetic aperture radar. Sci China Inf Sci, 2017, 60: 102305

3 Arias-Castro E, Eldar Y C. Noise folding in compressed sensing. IEEE Signal Process Lett, 2011, 18: 478–481

4 Candes E J, Wakin M B, Boyd S P. Enhancing sparsity by reweighted l_1 minimization. J Fourier Anal Appl, 2007, 14: 877–905

5 Haupt J, Castro R M, Nowak R. Distilled sensing: adaptive sampling for sparse detection and estimation. IEEE Trans Inform Theor, 2011, 57: 6222–6235

6 Peter S, Artina M, Fornasier M. Damping noise-folding and enhanced support recovery in compressed sensing. IEEE Trans Signal Process, 2015, 63: 5990–6002

7 Zhang Y, Zhang G, Wen F. Adaptive selective compressive sampling for sparse signal acquisition in noisy background. Electron Lett, 2015, 51: 1704–1706

8 Lavrenko A, Romer F, Galdo G D, et al. On the SNR variability in noisy compressed sensing. IEEE Signal Process Lett, 2017, 24: 1148–1152

9 Cai T T, Wang L. Orthogonal matching pursuit for sparse signal recovery with noise. IEEE Trans Inform Theor, 2011, 57: 4680–4688

10 Zhang S L, Xi F, Chen S Y, et al. Segment-sliding reconstruction of pulsed radar echoes with sub-Nyquist sampling. Sci China Inf Sci, 2016, 59: 122309

11 Quan X Y, Zhang B C, Wang Z D, et al. An efficient data compression technique based on BPDN for scattered fields from complex targets. Sci China Inf Sci, 2017, 60: 109302